The Stellar Populations of Lyman Break Galaxies at z~5

Kiyoto Yabe[1], Kouji Ohta[1], Ikuru Iwata[2], Marcin Sawicki[3]
Naoyuki Tamura[4], Masayuki Akiyama[4], Kentaro Aoki[4]

1. Kyoto Univ.
2. NAOJ, Okayama
3. St. Mary's Univ.
4. NAOJ, Hawaii

Abstract

We present the results of SED fitting analysis for Lyman Break Galaxies at z~5 in the GOODS-N and its flanking fields. With the IRAC images in the GOODS-N, which are publicly available, and the IRAC images that we observed in the flanking fields, we constructed the rest-frame UV-optical SEDs for our large sample that is selected robustly. For this sample, we fit the observed SEDs with population synthesis models. We found that there were a significant number of galaxies whose stellar masses are $>10^{10}$ M_{sun} at z~5. The comparison of the distribution of the parameters for our sample with that for the z=2-3 samples shows the increase of the stellar mass from z~5 to z=2-3 and that the z~5 galaxies are relatively younger than for the z=2-3 galaxies. We found that the color excess of our sample is larger, and thus, the star formation rate is higher than in z=2-3 galaxies. We conclude that the galaxies at z~5 are undergoing explosive star formation making them dusty. A large number of our sample galaxies that selected robustly allow us to derive the stellar mass function of LBGs at z~5. The stellar mass function for our sample agrees with that for the IRAC-selected sample of Elsner et al. 2007 but disagrees with that for the Ks-selected sample of Drory et al. 2005. By integrating down to $10^8 M_{sun}$, the cosmic stellar mass density at z~5 is calculated to be $7\times10^6 M_{sun} Mpc^{-3}$, i.e., about 1.4% of the local stellar mass density was assembled in the first 1.2Gyr. Compared with other observational works and theoretical predictions, the mass density of our sample is consistent with the general trend of the increase of the cosmic stellar mass density with time.

1. Objective

We examine the stellar populations of Lyman Break Galaxies(LBGs) at z~5 by Spectral Energy Distribution(SED) fitting analysis and its evolution from z~5 to z=2-3. With the advent of Spitzer, we can access the rest-frame optical properties of galaxies at z~5, which are sensitive to stellar mass of galaxies. In addition to the public IRAC/Spitzer data in the GOODS-N region, we obtained the IRAC images in the flanking fields (GOODS-FF), which makes our sample size large and allows us to determine the massive part of the stellar mass function of LBGs at z=5 robustly.

2. Sample Selection

We use the LBG sample of Iwata et al.(2007), which consists of ~600 objects around the GOODS-N. Among them, we select objects which appear to be isolated and not contaminated by neighboring objects in IRAC images. With the public IRAC images in the GOODS-N and the IRAC images we observed in the GOODS-FF, we constructed observed SEDs for the large sample selected robustly, which consists of ~100 objects.

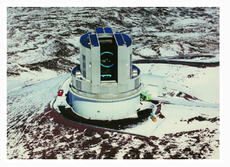

Subaru/Suprime-Cam
Effective area: ~500 arcmin^2
Magnitude limit (1.2"Φ, 5σ):
V:28.2, Ic:26.9, z':26.6

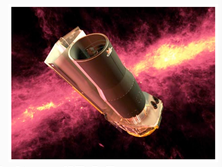

Spitzer/IRAC
Effective area: ~400 arcmin^2
Magnitude limit (2.4"Φ, 3σ):
3.6μm:25.9, 4.5μm: 25.6 (GOODS-N)
3.6μm:24.8, 4.5μm: 24.1 (GOODS-FF)

Area covered by IRAC is presented on the Subaru/Suprime-Cam area. Almost 80% of the optical images is covered by the mid-Infrared images.

In the bottom figure, two example images of our sample are shown. These objects are selected robustly to make reliable photometry.

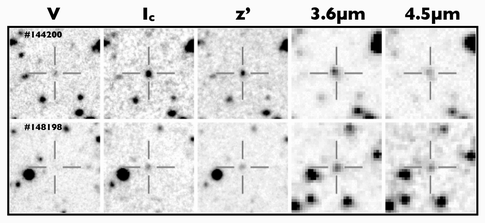

The postage stamps of objects in 5 passbands. The LBG candidate is indicated by a cross in each panel.

3. Population Synthesis Modeling

population synthesis modeling is handled as follows:

- Bruzual & Charlot 2003
- Salpeter IMF (0.1 - 100M_{sun})
- Constant Star Formation History
- 0.2 Z_{sun} model
- Calzetti extinction law
- Including Hα emission
- Redshift of all objects is fixed to be z=4.8

Note:
- Hα emission line is included in the model spectrum with Kennicutt law.
- We examine the effects of these model assumptions (choice of star formation history, metallicity, extinction law) on the stellar mass and found the effects is ~0.3dex at most.

4. Results

Comparing the observed SEDs with model SEDs, we infer the stellar properties of galaxies at z~5. In the bottom-left figure, a example of our fitting result is presented with the output parameters.

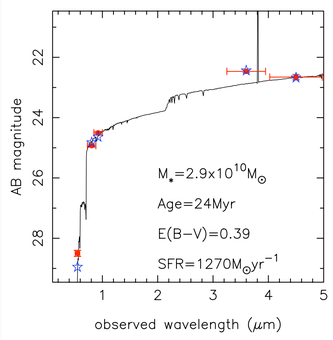

A best-fitted $0.2Z_{sun}$, CSF model. The observed SED and the model SED are indicated by red points and blue points, respectively. The best-fitted parameters are also shown.

Sample best-fitted parameters

$M_*^{median} = 3.8\times10^9 M_{sun}$
$Age^{median} = 25$ Myr
$E(B\text{-}V)^{median} = 0.23$ mag
$SFR^{median} = 190\ M_{sun}yr^{-1}$

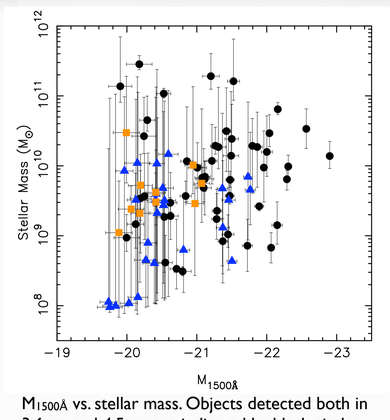

$M_{1500Å}$ vs. stellar mass. Objects detected both in 3.6μm and 4.5μm are indicated by black circles. Objects detected only in 3.6μm(4.5μm) are indicated by blue triangles(orange squares).

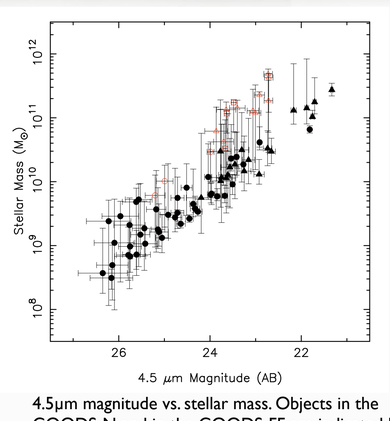

4.5μm magnitude vs. stellar mass. Objects in the GOODS-N and in the GOODS-FF are indicated by circle and triangle, respectively. Objects whose best-fitted age is larger than the cosmic age at z~5 are shown as red symbols.

In upper-left figure, $M_{1500Å}$ vs. stellar mass plot is presented. There appears to be a loose correlation between the rest-frame UV luminosity and stellar mass. In upper-right figure, a tight correlation between the rest-frame optical luminosity and stellar mass is shown.

5. Comparison with the results of z=2-3 galaxies

The distribution of the output parameters from the fitting of our sample is compared with those of z=2-3 sample in the right figure, where the histogram is normalized so that its peak value equals unity for comparison. For sample galaxies at z=2 and 3, we use Shapley et al. (2001) and Shapley et al. (2005), respectively.

Although the detailed algorithm of SED fitting procedure is different from us, both samples are fitted using models of Bruzual & Charlot (2003) with a Salpeter IMF, constant star formation history, and the Calzetti et al. (2001) extinction law. For the fair comparison, we use the samples whose the rest-frame UV absolute magnitudes are brighter than -19.7 mag.

The stellar mass of z~5 galaxies is smaller than that of z=2-3 galaxies by a factor of ~4 and the age of z~5 galaxies is relatively younger than that of z=2-3 galaxies. The amount of dust content is larger and the star formation rate is higher than in z=2-3.

We conclude from these comparisons that galaxies at z~5 are forming stars actively, and in consequence, they are dusty and dominated by young stellar populations.

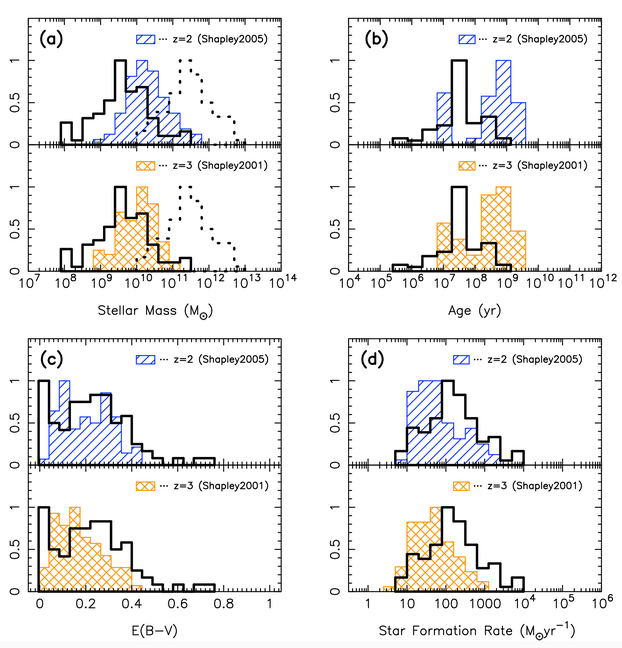

Distribution of best-fitted parameters for z~5 sample with that for z=3 sample from Shapley et al.(2001) and z=2 sample from Shapley et al.(2005). For comparison, peaks of the distribution are normalized to unity.

In the upper left panel of the upper right figure, the dotted line indicates the distribution of stellar mass at z=2 assuming that each galaxy of our sample continues the star formation at the rate derived from the SED fit until z=2. As a whole, the distribution shifts toward larger mass than observed at z=2. This implies that star formation may decrease from z~5 to z=2.

6. Comparison with the results of z=5-6 galaxies

The distribution of the output parameters from the fitting of our sample is compared with those of other z=5-6 samples. For sample galaxies at z=5, we use Stark et al. (2007) and Verma et al. (2007), for z=6 samples, we use Yan et al.(2006) and Eyles et al.(2007). The ranges of the rest-frame UV and optical luminosity for these samples are almost the same.

As illustrated in the left figure, the range of the inferred stellar mass for our sample is broadly consistent with other observations: the masses are widely distributed from $M_* = 10^8 M_{sun}$ to $10^{11} M_{sun}$. However, while the median of the stellar mass of our sample is consistent with Verma et al.(2007) and Stark et al. (2007), it is marginally smaller by a factor of 3-4 than that for z=6 objects of Yan et al.(2006) and Eyles et al.(2007).

This may be partly due to the insufficient number of the z=6 sample for considering the statistical properties. It is noteworthy that the models used in the SED fitting for the z=6 sample are slightly different from those we used. Thus, the difference of the distribution of stellar mass between z=5 and z=6 samples may not be significant.

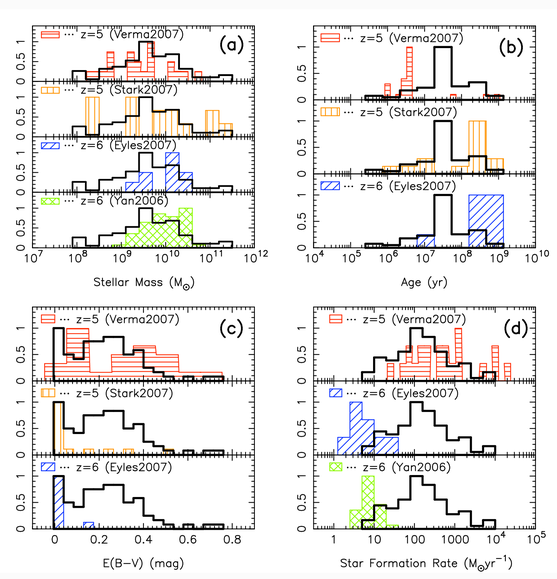

Distribution of best-fitted parameters for z~5 sample with that for samples of Stark et al.(2006), Verma et al.(2007), Yan et al.(2006), and Eyles et al.(2007). For comparison, peaks of the distribution are normalized to unity.

7. The Stellar Mass function / Mass Density

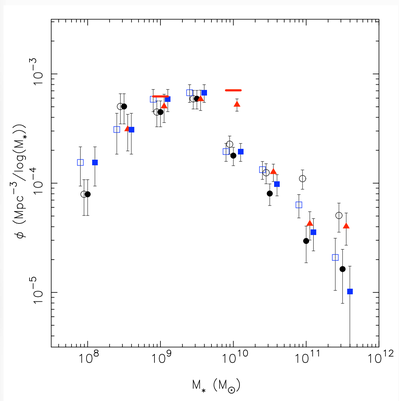

The stellar mass functions of LBGs at z~5 assuming various star formation histories (constant star formation: circle, instantaneous burst: triangle, τ-model: square). The mass function excluding objects whose fitted age is larger than the cosmic age at z=4.8 is indicated by filled symbols. The horizontal bars indicate the possible number densities including objects detected neither in 3.6μm nor 4.5μm.

The large sample of LBGs whose stellar mass is estimated robustly allows us to derive the stellar mass function of LBGs at z~5. The derived stellar mass functions assuming various star formation histories are plotted in the left figure. Although uncertainties remains, the stellar mass function we present in this work is that derived with constant star formation history and excluding objects whose fitted ages exceed the cosmic age at z~5.

As illustrated in the right figure, The stellar mass function for our sample is broadly consistent with that for the sample of Elsner et al.(2007) but disagrees with the results of Drory et al. (2005) in the low-mass end. Our results and theoretical models agree at the massive end but disagree at the low-mass end.

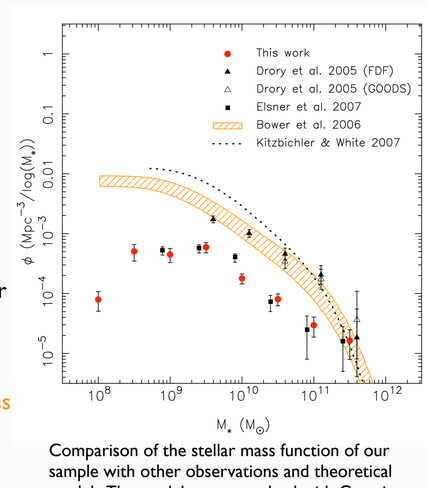

Comparison of the stellar mass function of our sample with other observations and theoretical models. The models are convolved with Gaussian with a s.d. of 0.3 dex considering measurement errors.

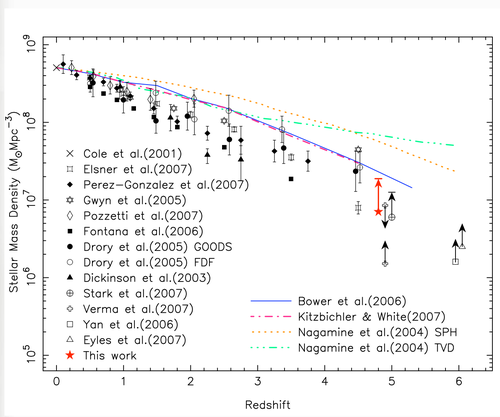

The cosmic stellar mass density as a function of redshift. The data point for our z~5 sample is plotted with other observations at various redshifts. Our result is indicated by a red star and the possible upper limit is shown with a horizontal bar. Also, theoretical predictions from semi-analytical models and hydrodynamics simulations are plotted with observed data. All observed values and models of Bower et al.(2006) and Kitzbichler & White(2007) are integrated down to $10^8 M_{sun}$. Note that two models of Nagamine et al.(2004) are total stellar mass densities.

By integrating the stellar mass function down to $M_*=10^8 M_{sun}$, the cosmic stellar mass density is calculated to be $7\times10^6 M_{sun} Mpc^{-3}$, which is about 1.4% of the local stellar mass density of Cole et al. (2001).

In the left figure, Comparison with observations and theoretical models is shown. All data points are values integrated down to $10^8 M_{sun}$ except for the models of Nagamine et al.(2004).

Our data point is consistent with the general trend of the increase of stellar mass density with time, which is underestimated with respect to the theoretical models, especially at high-z.